Low Intensity Vibration Restores Nuclear YAP Levels and Acute YAP Nuclear Shuttling in Mesenchymal Stem Cells Subjected to Simulated Microgravity

Thompson M[1], Woods K[2], Newberg, J[1], Oxford JT[2], Uzer G[1†]

[1] Mechanical and Biomedical Engineering, Boise State University

[2] Biomolecular Sciences Graduate Program, Boise State University

[†] Corresponding Author

Running title: LIV rescues SMG-inhibited YAP nuclear entry

Funding support: NASA ISGC NNX15AI04H, NIH R01AG059923, and 5P2CHD086843-03, P20GM109095, P20GM103408 and NSF 1929188.

[†] Corresponding author:

Gunes Uzer PhD

Boise State University

Department of Mechanical and Biomedical Engineering

1910 University Drive, MSd-2085

Boise, ID 83725-2085

Ph. (208) 426-4461

Email: gunesuzer@boisestate.edu

Abstract

Reducing the bone deterioration that astronauts experience in microgravity requires countermeasures that can improve the effectiveness of rigorous and time-expensive exercise regimens under microgravity. The ability of low intensity vibrations (LIV) to activate force-responsive signaling pathways in cells suggests LIV as a potential countermeasure to improve cell responsiveness to subsequent mechanical challenge. Mechanoresponse of mesenchymal stem cells (MSC) that maintains bone-making osteoblasts is in part controlled by the "mechanotransducer" protein YAP (Yes-associated protein) which is shuttled into the nucleus in response cyto-mechanical forces. Here, using YAP nuclear shuttling as a measure of MSC mechanoresponse, we tested the effect of 72 hours of simulated microgravity (SMG) and daily LIV application (LIV_{DT}) on the YAP nuclear entry driven by either acute LIV (LIV_{AT}) or Lysophosphohaditic acid (LPA), applied at the end of the 72h period. We hypothesized that SMG-induced impairment of acute YAP nuclear entry will be alleviated by daily application of LIV_{DT}. Results showed that while both acute LIV_{AT} and LPA treatments increased nuclear YAP entry by 50% and 87% over the basal levels in SMG-treated MSCs, nuclear YAP levels of all SMG groups were significantly lower than non-SMG controls. Daily dosing of LIV_{DT}, applied in parallel to SMG, restored the SMG-driven decrease in basal nuclear YAP to control levels as well as increasing the LPA-induced but not LIV_{AT}-induced YAP nuclear entry over the non-LIV_{DT} treated, SMG only, counterparts. These cell level observations suggest that utilizing daily LIV_{DT} treatments is a feasible countermeasure for increasing the YAP-mediated anabolic responsiveness of MSCs to subsequent mechanical challenge under SMG.

Key Words: Simulated Microgravity, Low Intensity Vibrations, YAP, Nucleus, Mesenchymal Stem Cells, Mechanosignaling

53 **Introduction**

54 The musculoskeletal deterioration which astronauts experience on long-term space missions
55 and the resulting increase of traumatic physical injury risk is in part due to the reduction of
56 mechanical loading on the musculoskeleton [1]. To alleviate the detrimental effects of unloading,
57 astronauts undergo long, intensive regimens of running and resistance training in orbit [2].
58 Despite these efforts, astronauts lose an average bone density of 1% for each month they
59 spend in space [3]. This loss necessitates new non-pharmacologic therapies in addition to
60 exercise to keep bones healthy during long-term space missions. In bone, tissue level response
61 to mechanical challenge is in part regulated by osteoblasts and osteocytes [4]. Both osteoblasts
62 and osteocytes in turn share a common progenitor: the mesenchymal stem cell (MSC).
63 Therefore, the growth and differentiation of MCSs in response to mechanical stimulation is
64 required for the maintenance and repair of bone [5]. It is for this reason that the MSCs are a
65 potential target for mechanical therapies aiming to alleviate bone loss in astronauts, injured
66 service personnel with long periods of bedrest, and physically inactive aged individuals [6].
67

68 To maintain healthy bone making cell populations, MSCs rely on environmental mechanical
69 signals inside the bone marrow niches and near bone surfaces. While the exact characteristics
70 of the mechanical environment in which MSCs exist remains to be quantified, it is known that
71 during habitual activities, our bones are subjected to combinations of complex loads including
72 strain, fluid shear, and acceleration, each of which is inseparable [7]. For example, during
73 moderate running, cortical bone can experience strains up to 2000με [8,9], which also generates
74 coupled fluid flow within canaliculi of up to 100μm/s [10]. The interior of bone is filled with bone
75 marrow with viscosities in the range of 400-800cP [11]. During moderate running, tibial
76 accelerations are within the 2-5g range [12] (1g = 9.81 m/s^2), creating a complex loading at the
77 bone-marrow interface that depends on many factors including frequency, amplitude, and
78 viscosity [13]. *In silico* studies reveal that when exposed to vibrations (0.1-2g), marrow-filled

79 trabecular compartments generate fluid shear stresses up to 2Pa [13,14], capable of driving bone
80 cell functions [15]. Interestingly, while these high magnitude forces are only experienced a few
81 times during the day, bones are bombarded by smaller mechanical signals arising from muscle
82 contractions that generate bone strains ranging between 2 to 10με [16]. Exogenous application of
83 small magnitude mechanical regimes in the form of low intensity vibrations (LIV) ranging
84 between 0.1-2g acceleration magnitudes and 20-200Hz frequencies were shown to be effective
85 in improving bone and muscle indices in clinical and preclinical studies [17]. At the cellular level,
86 our group has reported that application of LIV increases MSC contractility [18], activates RhoA
87 signaling [19], and results in increased osteogenic differentiation and proliferation of MSCs [20].
88
89 One of the most actively investigated signaling pathways that regulate the MSC
90 mechanoresponse is the Yes-associated protein (YAP) signaling pathway. YAP depletion in
91 stem cells results in reduced proliferation and osteogenesis [21,22]. Similarly, depleting YAP from
92 osteoblast progenitors decreases both bone quality and quantity in mice [23]. Functionally, in
93 response to cytomechanical forces and substrate stiffness, YAP moves from the cytoplasm to
94 the nucleus where it interacts with its co-transcriptional activators such as TEAD to regulate
95 gene expression related to proliferation [24]. For example, application of substrate strain induces
96 YAP nuclear entry and YAP transcriptional activity which is required to activate proliferation [25].
97 While it has been shown that YAP nuclear entry is triggered by soluble factors that increase F-
98 actin contractility such as Lysophosphatidic acid (LPA)[26,27], large changes in substrate stiffness
99 [22], or substrate stretch ranging from 3% to 15% [25,28], it is not known if low magnitude signals like
100 LIV also trigger acute YAP nuclear entry.
101
102 Research aimed at studying the effects of microgravity at the cellular level often relies on
103 simulated microgravity (SMG) devices designed to alter the gravitational conditions that cells
104 experience by rotating on one or multiple axes at low speed [29-31]. SMG decreases MSC

105 proliferation [32] and cytoskeletal contractility [29,33,34]. In this way, application of physical or soluble
106 factors that induce cytoskeletal contractility are commonly used as countermeasures for SMG
107 [35,36]. SMG also alters nuclear structure. Research from our group has shown that SMG results in
108 reduced levels of integral nuclear proteins such as Lamin A/C and LINC (Linker of
109 Nucleoskeleton and Cytoskeleton) complex elements Sun-2 [37]. As mechanically induced
110 nuclear shuttling of YAP and its paralog TAZ have been associated with LINC complex function
111 [38], SMG also results in decreased nuclear levels of the YAP paralog protein TAZ [35].
112 Interestingly, twice daily application of LIV for 20 minutes during SMG recovers both MSC
113 proliferation and levels of nuclear envelope proteins LaminA/C and Sun-2, suggesting LIV as a
114 potential countermeasure to improve YAP-mediated mechanosignaling in MSCs under SMG.
115
116 In this study, using YAP nuclear shuttling as a measure of MSC mechanoresponse, we tested
117 the effect of 72 hours of simulated microgravity (SMG) and daily LIV application (LIV_{DT}) on the
118 YAP nuclear entry driven by either acute LIV (LIV_{AT}) or Lysophosphohaditic acid (LPA), applied
119 at the end of the 72h period. We hypothesized that SMG-induced impairment of YAP nuclear
120 entry in response to mechanical and soluble factors will be alleviated by daily application of LIV.
121
122 **Results**
123 *Acute LIV_{AT} application increases nuclear YAP levels*
124 To quantify the acute YAP nuclear entry in response to LIV, MSCs were plated at density of
125 1,700 cells/cm^2 and were allowed to attach for 24hr. Following this, MSCs were subjected to
126 treatment in two groups: control and acute LIV treatment regimen (LIV_{AT}). The LIV_{AT} regimen
127 consisted of 5x 20min vibration periods separated by 1hr in between each repetition at room
128 temperature while control samples were treated identically (also taken out of the incubator) but
129 were not vibrated. Immediately after LIV_{AT}, samples were immunostained for YAP and DAPI
130 was used to visualize the nucleus. MATLAB was used to quantify the changes in the nuclear

131 YAP levels. As shown in **Fig.1a**, confocal images showed an increase in YAP staining in the cell
132 nuclei. Analysis of confocal images to quantify nuclear YAP intensity shown in **Fig.1b** revealed
133 a 32% increase in the nuclear YAP levels in the LIV_{AT} samples as compared to the control
134 samples ($p<0.0001$). As both LIV-induced focal adhesion signaling [19] and YAP nuclear entry in
135 response to substrate strain [28] requires intact LINC function, disabling LINC function via a
136 dominant negative overexpression of Nesprin KASH (Klarsicht, ANC-1, Syne homology)
137 fragment both decreased basal nuclear YAP levels by 34% ($p<0.0001$) and impeded the LIV-
138 induced YAP nuclear entry when compared to empty plasmid (**Fig.S1**).
139
140 *Basal nuclear YAP levels decreased by SMG were rescued by daily application of LIV_{DT}*
141 We next tested whether SMG decreases basal YAP levels and whether a daily LIV treatment
142 regimen (LIV_{DT}), applied in parallel with SMG, could alleviate decreased YAP in the nucleus. As
143 we reported previously, LIV_{DT} consisting of 2x 20min vibrations applied every 24 hours during
144 the 72h period of SMG application was effective at restoring MSC proliferation and whole cell
145 YAP levels, when applied in conjunction with SMG [37]. MSCs were plated at a density of 1,700
146 cells/cm^2 in 25 cm^2 tissue culture SlideFlasks (Nunc, #170920) and were allowed to attach for
147 24h, after which point, the flasks were filled completely with growth medium, sealed, and
148 subjected to 72h of treatment followed by immunostaining for YAP and nuclear staining using
149 DAPI. During the 72h treatment period, MSCs were divided into three groups: control samples,
150 SMG samples which were subjected to the standard regimen of 72h of continuous SMG, and
151 SMG+LIV_{DT} samples which were subjected to both the 72h SMG regimen and the daily LIV_{DT}
152 regimen. Representative images for YAP and DAPI stained images are shown in **Fig.2a.** As
153 depicted in **Fig.2b**, quantitative analysis of confocal images revealed a 42% decrease in the
154 nuclear YAP intensity in the SMG-treated samples as compared to the control samples
155 ($p<0.0001$). Compared to the SMG group, nuclear YAP levels of the LIV_{DT} treated MSCs

156 showed an increase of 67%, respectively. There was no significant nuclear YAP level difference
157 between of LIV_{DT} treated MSCs and non-SMG controls.
158
159 *LIV_{AT}-induced YAP nuclear entry decreased by SMG was not restored by daily LIV_{DT} application*
160 As SMG decreased basal nuclear YAP levels, we next tested whether SMG decreases LIV_{AT}-
161 induced YAP mechanosignaling (i.e. nuclear shuttling). Since LIV_{DT} was able to restore nuclear
162 YAP levels (**Fig.2**), the SMG+LIV_{DT} group was added to evaluate the effect of LIV_{DT} on the SMG
163 response. A schematic of the experimental design is given in **Fig.3**. MSCs were divided into six
164 groups in which the CTRL, SMG, SMG+LIV_{DT} groups were treated with ±LIV_{AT} at the end of 72h
165 and nuclear YAP levels were measured As shown in **Fig.4**, SMG alone decreased basal nuclear
166 YAP levels by 37% ($p<0.0001$) which were restored back to control levels in the SMG+LIV_{DT}
167 group. As depicted in **Fig.4**, +LIV_{AT} increased nuclear YAP levels in the CTRL, SMG and
168 SMG+LIV_{DT} groups by 50%, 69% and 22%, respectively ($p<0.0001$) while exhibiting the smallest
169 increase in the SMG+LIV_{DT}. As a result, final nuclear YAP levels in the SMG+LIV_{DT}+LIV_{AT} group
170 was not significantly different from the SMG+LIV_{AT} and 23% lower than the LIV_{AT} group
171 ($p<0.0001$).
172
173 *LPA treatment increases nuclear YAP levels*
174 As SMG+LIV_{DT} treatment did not improve the acute LIV_{AT} response when compared to the SMG
175 group, we next considered a soluble regulator of cytoskeletal tension, LPA. To test the effect of
176 LPA on the acute YAP nuclear entry, two LPA concentrations (50μM and 100μM) were
177 compared against control samples. Shown in **Fig.5**, nuclear YAP levels were almost doubled
178 under a two-hour exposure to 50μM LPA and 100μM LPA treatments with 99% and 107%
179 increases as compared to the control samples ($p<0.0001$). Nuclear YAP levels for 50μM LPA
180 and 100μM LPA treatments were not significantly different. Therefore, we chose to use 50μM
181 LPA treatment in the subsequent experiments.

182

183 *LPA-induced YAP nuclear entry decreased by SMG was alleviated by daily LIV_{DT} application*

184 In order to evaluate whether LIV_{DT} can restore LPA-induced YAP mechanosignaling after SMG,
185 50μM LPA dissolved in DMSO or DMSO as vehicle control were added to the samples at the
186 end of the 72h treatment of either CTRL, SMG or SMG+LIV_{DT} treatments. The CTRL group,
187 SMG group, and SMG+LIV_{DT} group were subjected to the same treatment as in the previous
188 experiments and displayed similar results. As depicted in **Fig.6**, +LPA increased nuclear YAP
189 levels in the CTRL, SMG and SMG+LIV_{DT} groups by 105%, 67% and 43% respectively
190 ($p<0.0001$). While final YAP nuclear levels in SMG+LIV_{DT}+LPA remained 70% higher than
191 SMG+LPA group ($P<0.0001$), it remained 29% lower than the LPA group ($P<0.0001$).

192

193 *Nuclear stiffness and area were not affected by SMG and SMG+LIV_{DT} treatments.*

194 As YAP mechanosignaling of SMG+LIV_{DT} MSCs remained below control levels in response to
195 both LIV_{AT} and LPA, we quantified the nuclear stiffness in CTRL, SMG and SMG+LIV_{DT}
196 samples. AFM testing was used to quantify the elastic modulus of the nucleus by measuring
197 load-displacement curves on top of the nucleus. As shown in **Fig.7a**, analysis revealed no
198 statistically significant effect on nuclear elastic modulus in the SMG or SMG+LIV_{DT} groups
199 compared to control levels. We have further quantified nuclear area as a measure of cyto-
200 mechanical forces on the nucleus [39]. Shown in **Fig.7b**, analysis of cross-sectional area of cell
201 nuclei using DAPI stained images revealed no significant effect on average nuclear size by
202 either SMG or combined SMG+LIV_{DT} treatment compared to control levels.

203

204 **Discussion**

205 The mechanical forces to which the bone and muscle tissue cells of the human body are
206 subjected both on Earth and in microgravity environments are complex and remain incompletely
207 understood. At the same time, it is clear that these forces are required for healthy tissue growth

208 on Earth. The complexity of these forces makes it difficult to design realistic experiments that
209 comprehensively simulate *in vivo* conditions. While the *in vitro* experiments utilizing SMG and
210 LIV treatments used in this study are limited in this way and do not entirely correlate with the
211 physiological behavior of these cells *in vivo*, the experiments presented here remain useful for
212 testing cell behavior under well-defined conditions.
213
214 In this study, we focused on YAP mechanosignaling in MSCs. The first experiments
215 demonstrated that repeated LIV_{AT} application over six hours was capable of stimulating YAP
216 entry into the nucleus (**Fig.1**). These findings suggest that similar to high magnitude substrate
217 strains [25] smaller mechanical signals such as LIV can be effective at increasing nuclear YAP
218 levels. Further, in agreement with earlier reports utilizing uniaxial strain [28], LIV_{AT}-induced
219 increase in nuclear YAP levels also required functional LINC complexes (**Fig.S1**). In these
220 experiments, we did not compare LIV_{AT} with strain because the application of 5 to 15% stretch
221 onto sealed culture flasks was not technically possible without significantly altering experimental
222 conditions. Instead, LPA addition served as the best option for applying a simple mechanical
223 stimulation in order to evaluate the YAP mechanotransduction. LPA is a phospholipid derivative
224 signaling molecule which is capable of causing the simulation of static transient stretch of a cell
225 by increasing the contractility of the cytoskeleton [20,40]. The first experiments with LPA served to
226 verify that the simulation of stretch via increased cytoskeleton contractility was capable of
227 triggering YAP entry into the nucleus and the analysis methods utilized here were capable of
228 detecting this response (**Fig.5**).
229
230 The first SMG experiments confirmed a clear decrease in basal nuclear YAP levels.
231 Interestingly, SMG treated cells remained responsive, as both LIV_{AT} and LPA treatments were
232 able to increase the nuclear YAP levels at the end of acute stimulation period (< 6h). However,
233 final nuclear YAP levels in SMG treated MSCs remained significantly lower when compared to

234 non-SMG groups (**Fig.2, 4 & 6**). These findings suggested that the YAP mechanosignaling
235 apparatus of MSCs, to some extent, was intact under SMG. When applied in parallel to SMG,
236 daily LIV_{DT} treatment was able to restore basal YAP levels in the cell nucleus (**Fig.2**) measured
237 24h after the final LIV_{DT} treatment. This increase in nuclear levels supported our earlier report
238 that showed sustained recovery of MSC proliferation by LIV_{DT} [37].
239
240 Interestingly, this increase in basal nuclear YAP levels under LIV_{DT} was accompanied by a
241 reduced MSC response to LIV_{AT} treatment (**Fig.5**). When SMG+LIV_{DT} treated MSCs were
242 subjected to LIV_{AT}, the increase in nuclear YAP from the non-LIV_{AT} control was only 22%
243 ($p<0.0001$), which was small compared to the 77% increase seen in the SMG groups in
244 response to LIV_{AT}. As a result of this smaller increase in the SMG+LIV_{DT} group, there was no
245 measurable difference between SMG and SMG+LIV_{DT}, samples that were subjected to LIV_{AT}. It
246 has been previously reported that an application of multiple LIV bouts separated by a refractory
247 period is more effective at activating mechano-signaling pathways such as βcatenin [41]. It is
248 possible that long term application of LIV_{DT} results in cell structural adaptations that serve to
249 reduce MSC responsiveness to LIV_{AT} treatment. To test this possibility, we have replaced LIV_{AT}
250 with an LPA treatment. When LIV_{AT} was replaced by LPA treatment (**Fig.6**), responsiveness of
251 SMG+LIV_{DT} treated MSCs almost doubled to 43% (compared to 22% in response to LIV_{AT}) and
252 was significantly higher than the SMG+LPA group ($p<0.0001$), suggesting that LIV_{DT} increases
253 the YAP-mechanosignaling in response to LPA.
254
255 Absolute nuclear YAP intensity in the SMG+LIV_{DT}+LIV_{AT} group however, remained below the
256 LIV_{AT} group ($p<0.0001$). Previously published findings using the same treatment protocols
257 suggested that the total cellular YAP levels decreased by SMG were restored to control levels
258 by daily LIV [37]. This would indicate that total availability of YAP protein was not responsible for
259 this difference between the SMG+LIV_{DT}+LIV_{AT} and the LIV_{AT} groups. In regards to other

260 potential effects of SMG on the components of the mechanosignaling mechanism, one current
261 prevailing hypothesis suggests a role for nuclear pore opening in response to cyto-mechanical
262 forces [38] which may be affected by changes in the nuclear stiffness. To test this possibility, we
263 have performed additional AFM and imaging experiments. While the AFM measured nuclear
264 stiffness was 24% lower in SMG and SMG+LIV_{DT} groups on average, we were unable to identify
265 any statistically significant effects of SMG or LIV_{DT} treatment on nuclear stiffness or on nuclear
266 area (**Fig.7**). While our results were not able to detect any changes in nuclear stiffness,
267 considering the significant role that the nuclear membrane plays as a mechanical structural
268 component in the cell's interpretation of mechanical stimulus [42,43], more detailed future studies
269 are needed to study the effects of sMG on the nuclear envelope and nuclear structure.
270
271 In summary, while the restoration of basal nuclear levels and improvement of LPA induced YAP
272 nuclear entry under daily LIV_{DT} treatment identify LIV as a possible countermeasure to improve
273 MSC response under the detrimental effects of simulated microgravity, future studies are
274 required to understand why acute YAP nuclear entry in response to mechanical and soluble
275 factors remain less responsive.
276
277 **Methods and Materials**
278 *Mesenchymal Stem Cell Culture*
279 Primary mouse bone marrow derived MSC's were extracted as previously described[37,44]. MSCs
280 were then subcultured and plated in Iscove modified Dulbecco's cell culture medium (IMDM,
281 12440053, Gibco) with 10% fetal calf serum (FCS, S11950H, Atlanta Biologicals) and 1%
282 pen/strep. MSCs were subcultured in 55cm^2 culture dishes at a density of 1,300cells/cm^2.
283 Experimental cells were plated in SlideFlasks at density of 1,700cells/cm^2 and given 24h to
284 attach to the slide prior to experiments. Cell passages for MSCs used for experiments were
285 limited to P7-P15.

286

287 *Low Intensity Vibrations Treatment*

288 SlideFlasks with plated MSCs were filled completely with culture medium and placed in LIV
289 device designed and used in previous research (**Fig.3**) (Touchstone 2019). LIV device
290 subjected cells to low intensity 90 Hz lateral vibrations at 0.7g at room temperature. MSCs were
291 vibrated for 20min intervals separated over time. LIV_{AT} regimen was applied after 72h treatment
292 period and consisted of 5x 20min LIV with an hour in between each. Daily LIV_{DT} regimen
293 consisted of 3x treatments in parallel with SMG treatment each consisting of 2x 20min LIV with
294 2h in between.

295

296 *Simulated Microgravity Treatment*

297 SlideFlasks (Nunc, #170920) with plated MSCs were filled completely with culture medium
298 (**Fig.3**) and placed in a clinostat SMG device. The clinostat shown is a redesign of a custom-
299 made clinostat described in previous research (Touchstone, 2019) with a new flask holder
300 casing capable of holding SlideFlasks and is also autoclavable. The clinostat was used to
301 subject the MSCs to constant 15 RPM SMG for 72h.

302

303 *Immunofluorescence Staining and Image Analysis*

304 Immediately after mechanical treatment, MSCs plated in Slideflasks were removed from
305 treatment, and the SlideFlasks were disassembled in order to stain the MSCs on the slides
306 (**Fig.3**). The MSCs were fixed with 4% paraformaldehyde, then washed and permeabilized with
307 0.05% Triton X-100 in PBS, followed by immunostaining with YAP specific antibody (YAP
308 (D8H1X) Rabbit mAb, Cell Signaling Technologies) and Alexa Fluor red secondary antibodies
309 (Donkey anti-Rabbit IgG (H+L) Cross-Adsorbed Secondary Antibody, Alexa Fluor Plus 594 for
310 all experiments prior to usage of LPA. Subsequently, Donkey anti-Rabbit IgG (H+L) Cross-
311 Adsorbed Secondary Antibody, Alexa Fluor Plus 633 was used). Nuclear DNA was labeled via

312 DAPI (Vectashield Mounting Medium, Vector Laboratories). Stained samples were imaged with
313 a Leica TCS SP8 confocal microscope (40x, HC PL APO CS2 Oil Immersion) prior to usage of
314 LPA, after this Zeiss LSM 510 Meta Confocal Microscope (40x, HC PL APO CS2 Oil
315 Immersion) . Exported images were used to quantify relative YAP levels within each nuclei
316 (nuclear regions traced by DAPI stained nucleus) via custom-made MATLAB program (The
317 MathWorks, Natick, MA). DAPI images were analyzed using an edge-detection algorithm in
318 order to determine the nuclear area for each cell. The nuclear outline was then used as a mask
319 to quantify the average pixel intensity of the YAP stain within the nuclei of each individual cell.
320 (n=50-100 nuclei/sample).
321
322 *Atomic Force Microscopy*
323 Bruker Dimension FastScan AFM was used for collection of the atomic force measurements.
324 Tipless MLCT-D probes with a 0.03 N/m spring constant were functionalized with 10 μm
325 diameter borosilicate glass beads for force collection. The AFM's optical microscope was used
326 to locate individual live MSCs plated on the SlideFlask slides with the flask section removed for
327 access to the cells. The nucleus of each cell was tested with at least 3 seconds of rest between
328 each test. In each test, three force-displacement curves were obtained (ramping rate: 2 μm/sec
329 over 2 μm total travel, 1 μm approach, 1 μm retract), which were analyzed using Nanoscope
330 software with the implementation of a best-fit curve to a Hertzian (spherical) model (optimized
331 such that R^2 value was greater than 0.95, or $p<0.05$) to obtain elastic moduli of nuclear
332 membrane of individual nuclei.
333
334 *Statistical analysis*
335 All data analysis results were displayed graphically based on the mean value with standard
336 error bars. Differences between treatments were not assumed to follow a Gaussian distribution.
337 Therefore, group differences were identified via either non-parametric two-tailed Mann-Whitney

U-test (**Fig.1a**) or Kruskal-Wallis test followed by Tukey multiple comparison (**Fig.2b, 4, 5, 6, 7, &S1**). P-values of less than 0.05 were considered significant.

Data availability

The datasets generated and/or analyzed during the current study are available from the corresponding author on reasonable request.

Acknowledgements

This study was supported by NASA ISGC NNX15AI04H, NIH R01AG059923, and 5P2CHD086843-03, P20GM109095, P20GM103408 and NSF 1929188.

Competing interests

The author(s) declare no competing interests, financial or otherwise.

Contributions

Thompson, M experimental methods, data analysis/interpretation, manuscript writing, final approval of manuscript.

Woods, K data analysis/interpretation, final approval of manuscript.

Newberg, J experimental methods, final approval of manuscript

Oxford JT, financial support, final approval of manuscript

Uzer, G concept/design, financial support, data analysis/interpretation, manuscript writing, final approval of manuscript

References

1 Smith, S. M. *et al.* Calcium metabolism before, during, and after a 3-mo spaceflight: kinetic and biochemical changes. *Am J Physiol* **277**, R1-10 (1999).

2 Greenleaf, J. E., Bulbulian, R., Bernauer, E. M., Haskell, W. L. & Moore, T. Exercise-training protocols for astronauts in microgravity. *Journal of applied physiology (Bethesda, Md. : 1985)* **67**, 2191-2204, doi:10.1152/jappl.1989.67.6.2191 (1989).

3 Vico, L. *et al.* Effects of long-term microgravity exposure on cancellous and cortical weight-bearing bones of cosmonauts. *Lancet (London, England)* **355**, 1607-1611 (2000).

4 Thompson, W. R., Rubin, C. T. & Rubin, J. Mechanical regulation of signaling pathways in bone. *Gene* **503**, 179-193, doi:10.1016/j.gene.2012.04.076 (2012).

5 Ozcivici, E. *et al.* Mechanical signals as anabolic agents in bone. *Nature reviews. Rheumatology* **6**, 50-59, doi:10.1038/nrrheum.2009.239 (2010).

6 Rando, T. A. & Ambrosio, F. Regenerative Rehabilitation: Applied Biophysics Meets Stem Cell Therapeutics. *Cell Stem Cell* **22**, 306-309, doi:10.1016/j.stem.2018.02.003 (2018).

7 Chan, M. E., Uzer, G. & Rubin, C. The Potential Benefits and Inherent Risks of Vibration as a Non-Drug Therapy for the Prevention and Treatment of Osteoporosis. *Current osteoporosis reports*, 1-9, doi:10.1007/s11914-012-0132-1 (2013).

8 Judex, S., Gross, T. S. & Zernicke, R. F. Strain Gradients Correlate with Sites of Exercise-Induced Bone-Forming Surfaces in the Adult Skeleton. *Journal of Bone and Mineral Research* **12**, 1737-1745, doi:10.1359/jbmr.1997.12.10.1737 (1997).

9 Rubin, C. T. & Lanyon, L. E. Dynamic strain similarity in vertebrates; an alternative to allometric limb bone scaling. *Journal of Theoretical Biology* **107**, 321-327, doi:10.1016/s0022-5193(84)80031-4 (1984).

10 Price, C., Zhou, X. Z., Li, W. & Wang, L. Y. Real-Time Measurement of Solute Transport Within the Lacunar-Canalicular System of Mechanically Loaded Bone: Direct Evidence for Load-Induced Fluid Flow. *Journal of Bone and Mineral Research* **26**, 277-285, doi:10.1002/jbmr.211 (2011).

11 Gurkan, U. A. & Akkus, O. The Mechanical Environment of Bone Marrow: A Review. *Annals of biomedical engineering* **36**, 1978-1991, doi:10.1007/s10439-008-9577-x (2008).

12 Vainionpaa, A. *et al.* Intensity of exercise is associated with bone density change in premenopausal women. *Osteoporosis international : a journal established as result of cooperation between the European Foundation for Osteoporosis and the National Osteoporosis Foundation of the USA* **17**, 455-463, doi:10.1007/s00198-005-0005-x (2006).

13 Dickerson, D. A., Sander, E. A. & Nauman, E. A. Modeling the mechanical consequences of vibratory loading in the vertebral body: microscale effects. *Biomechanics and Modeling in Mechanobiology* **7**, 191-202, doi:10.1007/s10237-007-0085-y (2008).

14 Coughlin, T. R. & Niebur, G. L. Fluid shear stress in trabecular bone marrow due to low-magnitude high-frequency vibration. *Journal of biomechanics* **45**, 2222-2229, doi:10.1016/j.jbiomech.2012.06.020 (2012).

15 Riddle, R. C. & Donahue, H. J. From Streaming Potentials to Shear Stress: 25 Years of Bone Cell Mechanotransduction. *Journal of Orthopaedic Research* **27**, 143-149, doi:10.1002/jor.20723 (2009).

16 Fritton, S. P., McLeod, K. J. & Rubin, C. T. Quantifying the strain history of bone: spatial uniformity and self-similarity of low-magnitude strains. *Journal of biomechanics* **33**, 317-325, doi:10.1016/s0021-9290(99)00210-9 (2000).

17 Pagnotti, G. M. *et al.* Combating osteoporosis and obesity with exercise: leveraging cell mechanosensitivity. *Nature Reviews Endocrinology*, doi:10.1038/s41574-019-0170-1 (2019).

18 Pongkitwitoon, S., Uzer, G., Rubin, J. & Judex, S. Cytoskeletal Configuration Modulates Mechanically Induced Changes in Mesenchymal Stem Cell Osteogenesis, Morphology, and Stiffness. *Scientific reports* **6**, 34791, doi:10.1038/srep34791 (2016).

19 Uzer, G. *et al.* Cell Mechanosensitivity to Extremely Low-Magnitude Signals Is Enabled by a LINCed Nucleus. *STEM CELLS* **33**, 2063-2076, doi:10.1002/stem.2004 (2015).

20 Uzer, G., Pongkitwitoon, S., Ete Chan, M. & Judex, S. Vibration induced osteogenic commitment of mesenchymal stem cells is enhanced by cytoskeletal remodeling but not fluid shear. *Journal of biomechanics* **46**, 2296-2302, doi:10.1016/j.jbiomech.2013.06.008 (2013).

21 Pan, J. X. *et al.* YAP promotes osteogenesis and suppresses adipogenic differentiation by regulating beta-catenin signaling. *Bone research* **6**, 18, doi:10.1038/s41413-018-0018-7 (2018).

22 Dupont, S. *et al.* Role of YAP/TAZ in mechanotransduction. *Nature* **474**, 179-183, doi:http://www.nature.com/nature/journal/v474/n7350/abs/10.1038-nature10137-unlocked.html#supplementary-information (2011).

23 Kegelman, C. D. *et al.* Skeletal cell YAP and TAZ combinatorially promote bone development. *FASEB journal : official publication of the Federation of American Societies for Experimental Biology* **32**, 2706-2721, doi:10.1096/fj.201700872R (2018).

24 Zhao, B. *et al.* TEAD mediates YAP-dependent gene induction and growth control. *Genes & development* **22**, 1962-1971, doi:10.1101/gad.1664408 (2008).

25 Benham-Pyle, B. W., Pruitt, B. L. & Nelson, W. J. Cell adhesion. Mechanical strain induces E-cadherin-dependent Yap1 and beta-catenin activation to drive cell cycle entry. *Science (New York, N.Y.)* **348**, 1024-1027, doi:10.1126/science.aaa4559 (2015).

26 Ho, L. T. Y., Skiba, N., Ullmer, C. & Rao, P. V. Lysophosphatidic Acid Induces ECM Production via Activation of the Mechanosensitive YAP/TAZ Transcriptional Pathway in Trabecular Meshwork Cells. *Investigative Ophthalmology & Visual Science* **59**, 1969-1984, doi:10.1167/iovs.17-23702 (2018).

27 Cai, H. & Xu, Y. The role of LPA and YAP signaling in long-term migration of human ovarian cancer cells. *Cell Communication and Signaling* **11**, 31, doi:10.1186/1478-811X-11-31 (2013).

28 Driscoll, Tristan P., Cosgrove, Brian D., Heo, S.-J., Shurden, Zach E. & Mauck, Robert L. Cytoskeletal to Nuclear Strain Transfer Regulates YAP Signaling in Mesenchymal Stem Cells. *Biophysical journal* **108**, 2783-2793, doi:10.1016/j.bpj.2015.05.010 (2015).

29 Janmaleki, M., Pachenari, M., Seyedpour, S. M., Shahghadami, R. & Sanati-Nezhad, A. Impact of Simulated Microgravity on Cytoskeleton and Viscoelastic Properties of Endothelial Cell. *Sci Rep* **6**, 32418, doi:10.1038/srep32418 (2016).

30 Qian, A. R. *et al.* Fractal Dimension as a Measure of Altered Actin Cytoskeleton in MC3T3-E1 Cells Under Simulated Microgravity Using 3-D/2-D Clinostats. *Biomedical Engineering, IEEE Transactions on* **59**, 1374-1380, doi:10.1109/TBME.2012.2187785 (2012).

31 Pardo, S. J. *et al.* Simulated microgravity using the Random Positioning Machine inhibits differentiation and alters gene expression profiles of 2T3 preosteoblasts. *Am J Physiol Cell Physiol* **288**, doi:10.1152/ajpcell.00222.2004 (2005).

32 Dai, Z. Q., Wang, R., Ling, S. K., Wan, Y. M. & Li, Y. H. Simulated microgravity inhibits the proliferation and osteogenesis of rat bone marrow mesenchymal stem cells. *Cell proliferation* **40**, 671-684, doi:10.1111/j.1365-2184.2007.00461.x (2007).

33 Shi, F. *et al.* Simulated Microgravity Promotes Angiogenesis through RhoA-Dependent Rearrangement of the Actin Cytoskeleton. *Cellular physiology and biochemistry : international journal of experimental cellular physiology, biochemistry, and pharmacology* **41**, 227-238, doi:10.1159/000456060 (2017).

464 34 Corydon, T. J. *et al.* Reduced Expression of Cytoskeletal and Extracellular Matrix Genes
465 in Human Adult Retinal Pigment Epithelium Cells Exposed to Simulated Microgravity.
466 *Cellular physiology and biochemistry : international journal of experimental cellular*
467 *physiology, biochemistry, and pharmacology* **40**, 1-17, doi:10.1159/000452520 (2016).
468 35 Chen, Z., Luo, Q., Lin, C., Kuang, D. & Song, G. Simulated microgravity inhibits
469 osteogenic differentiation of mesenchymal stem cells via depolymerizing F-actin to
470 impede TAZ nuclear translocation. *Scientific reports* **6**, 30322, doi:10.1038/srep30322
471 (2016).
472 36 Uddin, S. M. & Qin, Y. X. Enhancement of osteogenic differentiation and proliferation in
473 human mesenchymal stem cells by a modified low intensity ultrasound stimulation under
474 simulated microgravity. *PLoS One* **8**, e73914, doi:10.1371/journal.pone.0073914 (2013).
475 37 Touchstone, H. *et al.* Recovery of stem cell proliferation by low intensity vibration under
476 simulated microgravity requires intact LINC complex *npj. Microgravity* **5**,
477 doi:doi.org/10.1038/s41526-019-0072-5 (2019).
478 38 Shiu, J.-Y., Aires, L., Lin, Z. & Vogel, V. Nanopillar force measurements reveal actin-
479 cap-mediated YAP mechanotransduction. *Nature cell biology* **20**, 262-271,
480 doi:10.1038/s41556-017-0030-y (2018).
481 39 Saeed, M. & Weihs, D. Finite element analysis reveals an important role for cell
482 morphology in response to mechanical compression. *Biomechanics and Modeling in*
483 *Mechanobiology*, doi:10.1007/s10237-019-01276-5 (2019).
484 40 Riddick, N., Ohtani, K. & Surks, H. K. Targeting by myosin phosphatase-RhoA
485 interacting protein mediates RhoA/ROCK regulation of myosin phosphatase. *Journal of*
486 *Cellular Biochemistry* **103**, 1158-1170, doi:10.1002/jcb.21488 (2008).
487 41 Sen, B. *et al.* Mechanical signal influence on mesenchymal stem cell fate is enhanced by
488 incorporation of refractory periods into the loading regimen. *Journal of biomechanics* **44**,
489 593-599, doi:10.1016/j.jbiomech.2010.11.022 (2011).
490 42 De Magistris, P. & Antonin, W. The Dynamic Nature of the Nuclear Envelope. *Current*
491 *biology : CB* **28**, R487-r497, doi:10.1016/j.cub.2018.01.073 (2018).
492 43 Czapiewski, R., Robson, M. I. & Schirmer, E. C. Anchoring a Leviathan: How the
493 Nuclear Membrane Tethers the Genome. *Frontiers in genetics* **7**, 82,
494 doi:10.3389/fgene.2016.00082 (2016).
495 44 Uzer, G. *et al.* Sun-mediated mechanical LINC between nucleus and cytoskeleton
496 regulates betacatenin nuclear access. *Journal of biomechanics* **74**, 32-40,
497 doi:10.1016/j.jbiomech.2018.04.013 (2018).

498

499 **Figure 1. Acute LIV_{AT} application increases nuclear YAP levels**. (a) MSCs were subjected to
500 LIV_{AT} and stained with DAPI (blue) and YAP (red). Confocal images indicated an increased
501 nuclear YAP levels following acute LIV_{AT} applied as five 20min vibration periods separated by
502 1hr. (b) Quantitative analysis of confocal images showed a 32% of increase of nuclear YAP in
503 LIV_{AT} samples compared to controls. n>400/grp, group comparison was made a Mann-Whitney
504 U-test, *p<0.05, **p<0.01, ***p<0.01, ****p<0.0001.

505

506 **Figure 2. Basal nuclear YAP levels decreased by SMG were rescued by LIV_{DT}.** (a) MSCs
507 were subjected to SMG, and SMG+LIV_{DT} over 72h period and stained with DAPI (blue) and YAP
508 (red). (b) Quantitative analysis showed a 42% decrease of nuclear YAP levels in the SMG group
509 compared to control levels. The SMG+LIV_{DT} group showed a 67% increase of nuclear YAP
510 when compared to the SMG group. There was no statistically significant difference between
511 CTRL and SMG+LIV_{DT} groups. n>100/grp. Group comparisons were made via Kruskal-Wallis
512 test followed by Tukey multiple comparison, *p<0.05, **p<0.01, ***p<0.01, ****p<0.0001.
513
514 **Figure 3. Experimental design of combined SMG, LIV_{AT} and LIV_{DT} application.** MSCs were
515 subcultured and plated in SlideFlasks and allowed to attach for 24h before SlideFlasks were
516 filled with culture medium and sealed. Treatment regimen for MSC's involved 72h of SMG
517 (blue). LIV_{DT} regimen consisted of one treatment cycle every 24hr during SMG treatment with
518 each cycle consisting of 2x 20min LIV with an hour in between (yellow). LIV_{AT} regimen was
519 applied after 72h SMG treatment period and consisted of 5x 20min LIV with an hour in between
520 each (red). For LIV application, MSCs plated in SlideFlasks were placed in LIV device
521 constructed in the lab previous to this research. Vibrations were applied at peak magnitudes of
522 0.7 g at 90 Hz at room temperature. For SMG application, MSCs plated in SlideFlasks were
523 secured in lab custom-built clinostat inside incubator. The clinostat subjected the MSCs to
524 constant 15 RPM rotation simulated microgravity. After treatment, flask was removed for
525 immunofluorescence staining.
526
527 **Figure 4. LIV_{AT}-induced YAP nuclear entry decreased by SMG was not restored by daily**
528 **LIV_{DT} application.** MSCs were subjected to either CTRL, SMG, SMG+LIV_{DT} over 72h period
529 were subsequently treated with LIV_{AT}. Quantitative analysis of confocal images showed that
530 SMG alone decreased basal nuclear YAP levels by 37% which were increased back to control
531 levels in the SMG+LIV_{DT} group. +LIV_{AT} increased nuclear YAP levels in the CTRL, SMG and

532 SMG+LIV_{DT} groups by 50%, 69% and 22%, respectively. Nuclear YAP intensity in the
533 SMG+LIV_{DT}+LIV_{AT} group remained not significantly different from the SMG+LIV_{AT} and 23%
534 smaller than the LIV_{AT} group. n>200/grp. Group comparisons were made via Kruskal-Wallis test
535 followed by Tukey multiple comparison, *p<0.05, **p<0.01, ***p<0.01, ****p<0.0001.
536
537 **Figure 5. LPA treatment increases nuclear YAP levels.** MSCs were subjected to LPA
538 addition at 50μM and 100μM concentrations. Quantitative analysis of confocal images revealed
539 a 99% and a 107% increase in the 50μM LPA and 100μM LPA treatments compared to DMSO
540 treated controls, respectively. Nuclear YAP levels for 50μM LPA and 100μM LPA treatments
541 were not significantly different. n>30/grp. Group comparisons were made via Kruskal-Wallis
542 test followed by Tukey multiple comparison, *p<0.05, **p<0.01, ***p<0.01, ****p<0.0001.
543
544 **Figure 6. LPA-induced YAP nuclear entry decreased by SMG was alleviated by daily LIV_{DT}**
545 **application.** MSCs were subjected to SMG, and parallel SMG+LIV_{DT} over 72h period at the end
546 of 72h, samples were treated with either LPA (50μM) or DMSO. Quantitative analysis of
547 confocal images revealed that LPA addition increased nuclear YAP levels by 105%, 67% and
548 43% in the CTRL, SMG and SMG+LIV_{DT} when compared to DMSO controls. When compared to
549 nuclear YAP intensity of the LPA treatment alone, SMG+LPA and SMG+LIV_{DT}+LPA samples
550 were 55% and 29% lower, respectively. YAP nuclear levels in SMG+LIV_{DT}+LPA remained 70%
551 higher than SMG+LPA group. n>100/grp. Group comparisons were made via Kruskal-Wallis test
552 followed by Tukey multiple comparison, *p<0.05, **p<0.01, ***p<0.01, ****p<0.0001.
553
554 **Figure 7. Nuclear stiffness and area were not affected by SMG and SMG+LIV_{DT}**
555 **treatments.** MSCs were subjected to SMG, and parallel SMG+LIV_{DT} over 72h period. (a)
556 Compared to CTRL samples, AFM measured elastic modulus SMG and SMG+LIV treated
557 MSCs revealed an apparent decrease in elastic modules that were 21% and 27% below control

558 levels, measured differences were not statistically significant. n=10/grp (b) Quantitative analysis
559 of confocal images from the image groups revealed no significant effects of either SMG or LIV_{DT}
560 treatment on the average nucleus size. n=100/grp. Group comparisons were made via Kruskal-
561 Wallis test followed by Tukey multiple comparison, *p<0.05, **p<0.01, ***p<0.01, ****p<0.0001.
562
563 **Figure S1. LINC complex disruption decreases nuclear YAP levels and reduces LIV_{AT}-**
564 **induced YAP nuclear entry.** Plasmids harboring either a dominant negative KASH domain of
565 Nesprin (DNK) to disable LINC complex function or empty mCherry control (MC) were
566 overexpressed in MSCs. Following puromycin selection, MC or DNK expressing MSCs were
567 subjected to LIV_{AT}. Quantitative analysis of confocal images revealed a 49% increase of nuclear
568 YAP following LIV_{AT} in MC expressing control MSCs. Basal YAP levels of the DNK-CTRL group
569 was 34% lower compared to MC-CTRL and LIV_{AT} treatment failed to significantly increase
570 nuclear YAP over DNK-CTRL (18%, NS). n=30/grp, group comparisons were made via
571 Kruskal-Wallis test followed by Tukey multiple comparison, *p<0.05, **p<0.01, ***p<0.01,
572 ****p<0.0001.
573

Figure 1.

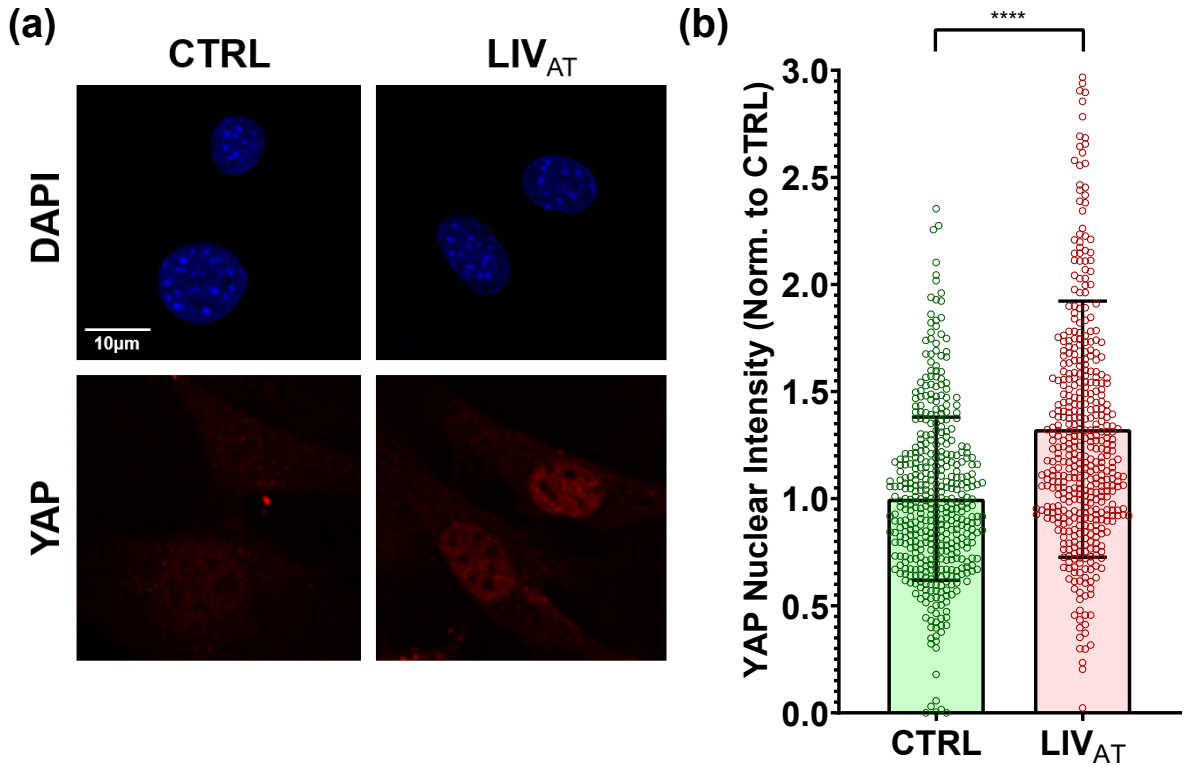

Figure 1. Acute LIV$_{AT}$ application increases nuclear YAP levels. (a) MSCs were subjected to LIV$_{AT}$ and stained with DAPI (blue) and YAP (red). Confocal images indicated an increased nuclear YAP levels following acute LIV$_{AT}$ applied as five 20min vibration periods separated by 1hr. (b) Quantitative analysis of confocal images showed a 32% of increase of nuclear YAP in LIV$_{AT}$ samples compared to controls. n>400/grp, group comparison was made a Mann-Whitney U-test, *p<0.05, **p<0.01, ***p<0.01, ****p<0.0001.

Figure 2.

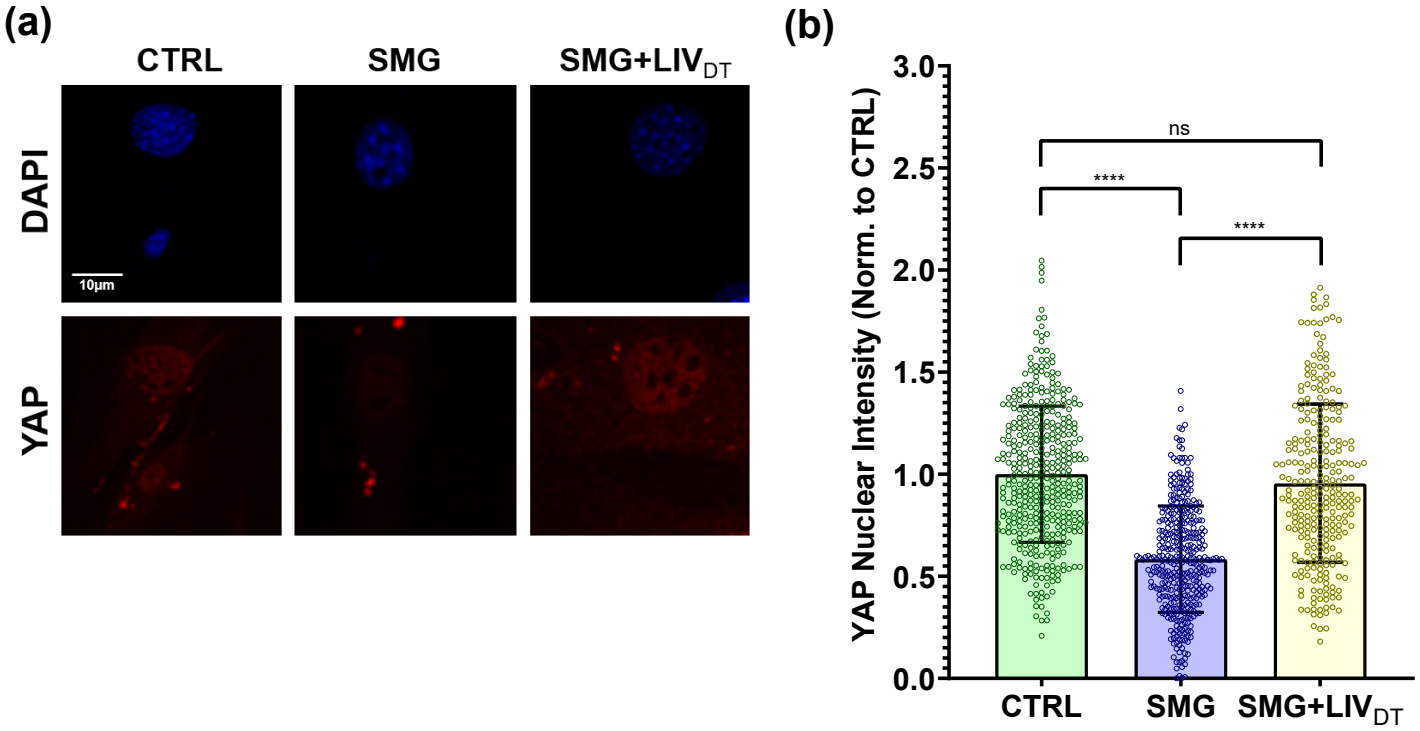

Figure 2. Basal nuclear YAP levels decreased by SMG were rescued by LIV$_{DT}$. (a) MSCs were subjected to SMG, and SMG+LIV$_{DT}$ over 72h period and stained with DAPI (blue) and YAP (red). (b) Quantitative analysis showed a 42% decrease of nuclear YAP levels in the SMG group compared to control levels. The SMG+LIV$_{DT}$ group showed a 67% increase of nuclear YAP when compared to the SMG group. There was no statistically significant difference between CTRL and SMG+LIV$_{DT}$ groups. n>100/grp. Group comparisons were made via Kruskal-Wallis test followed by Tukey multiple comparison, *p<0.05, **p<0.01, ***p<0.01, ****p<0.0001.

Figure 3.

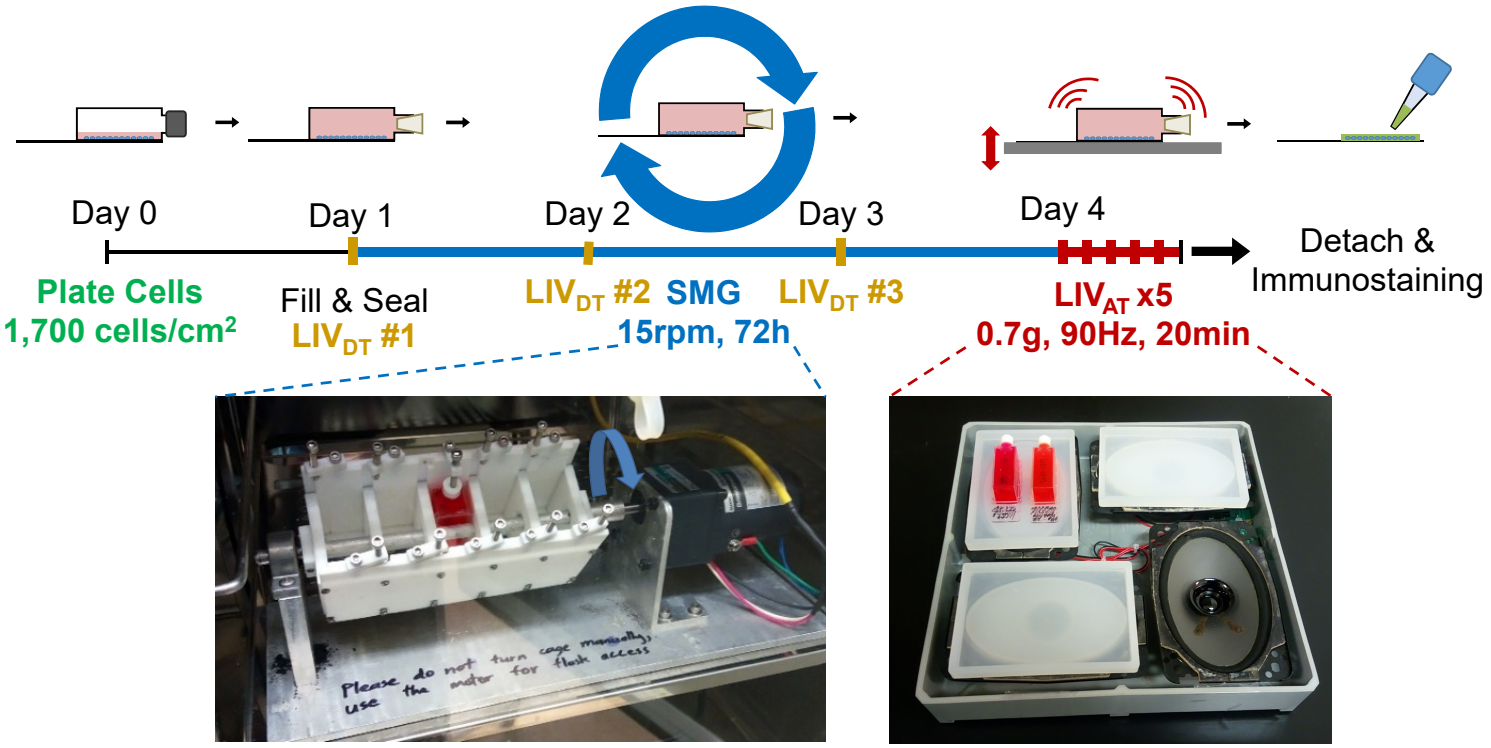

Figure 3. Experimental design of combined SMG, LIV_{AT} and LIV_{DT} application. MSCs were subcultured and plated in SlideFlasks and allowed to attach for 24h before SlideFlasks were filled with culture medium and sealed. Treatment regimen for MSC's involved 72h of SMG (blue). LIV_{DT} regimen consisted of one treatment cycle every 24hr during SMG treatment with each cycle consisting of 2x 20min LIV with an hour in between (yellow). LIV_{AT} regimen was applied after 72h SMG treatment period and consisted of 5x 20min LIV with an hour in between each (red). For LIV application, MSCs plated in SlideFlasks were placed in LIV device constructed in the lab previous to this research. Vibrations were applied at peak magnitudes of 0.7 g at 90 Hz at room temperature. For SMG application, MSCs plated in SlideFlasks were secured in lab custom-built clinostat inside incubator. The clinostat subjected the MSCs to constant 15 RPM rotation simulated microgravity. After treatment, flask was removed for immunofluorescence staining.

Figure 4.

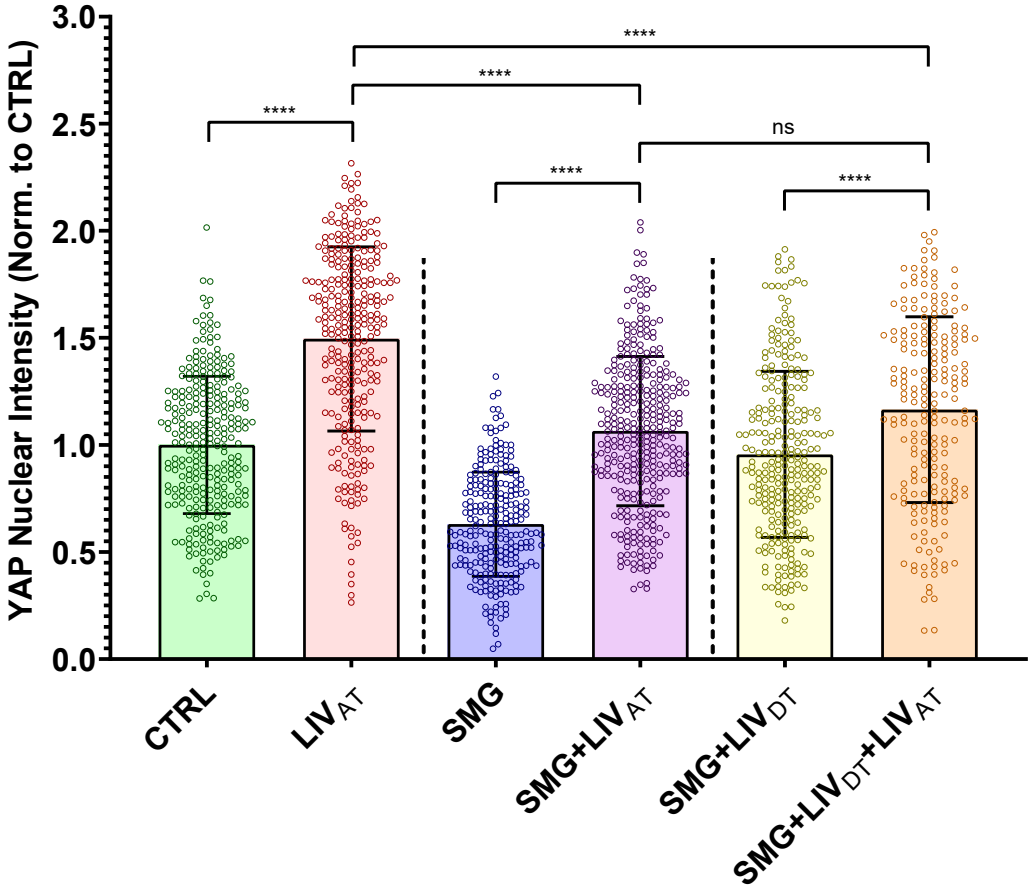

Figure 4. LIV_{AT}-induced YAP nuclear entry decreased by SMG was not restored by daily LIV_{DT} application. MSCs were subjected to either CTRL, SMG, SMG+LIV_{DT} over 72h period were subsequently treated with LIV_{AT}. Quantitative analysis of confocal images showed that SMG alone decreased basal nuclear YAP levels by 37% which were increased back to control levels in the SMG+LIV_{DT} group. +LIV_{AT} increased nuclear YAP levels in the CTRL, SMG and SMG+LIV_{DT} groups by 50%, 69% and 22%, respectively. Nuclear YAP intensity in the SMG+LIV_{DT}+LIV_{AT} group remained not significantly different from the SMG+LIV_{AT} and 23% smaller than the LIV_{AT} group. n>200/grp. Group comparisons were made via Kruskal-Wallis test followed by Tukey multiple comparison, *p<0.05, **p<0.01, ***p<0.01, ****p<0.0001.

Figure 5.

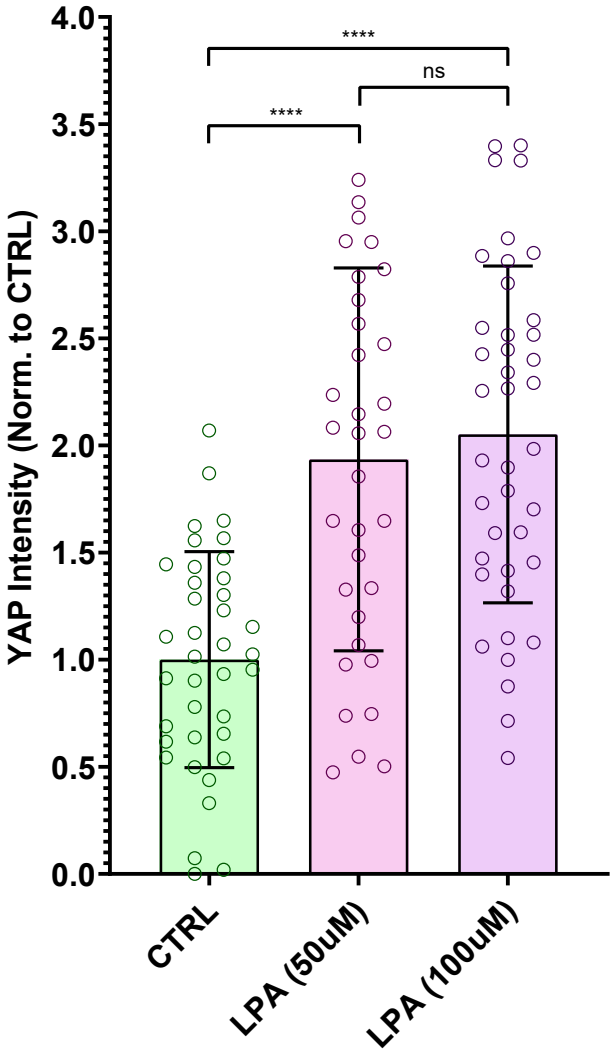

Figure 5. LPA treatment increases nuclear YAP levels. MSCs were subjected to LPA addition at 50μM and 100μM concentrations. Quantitative analysis of confocal images revealed a 99% and a 107% increase in the 50μM LPA and 100μM LPA treatments compared to DMSO treated controls, respectively. Nuclear YAP levels for 50μM LPA and 100μM LPA treatments were not significantly different. n>30/grp. Group comparisons were made via Kruskal-Wallis test followed by Tukey multiple comparison, *p<0.05, **p<0.01, ***p<0.01, ****p<0.0001.

Figure 6.

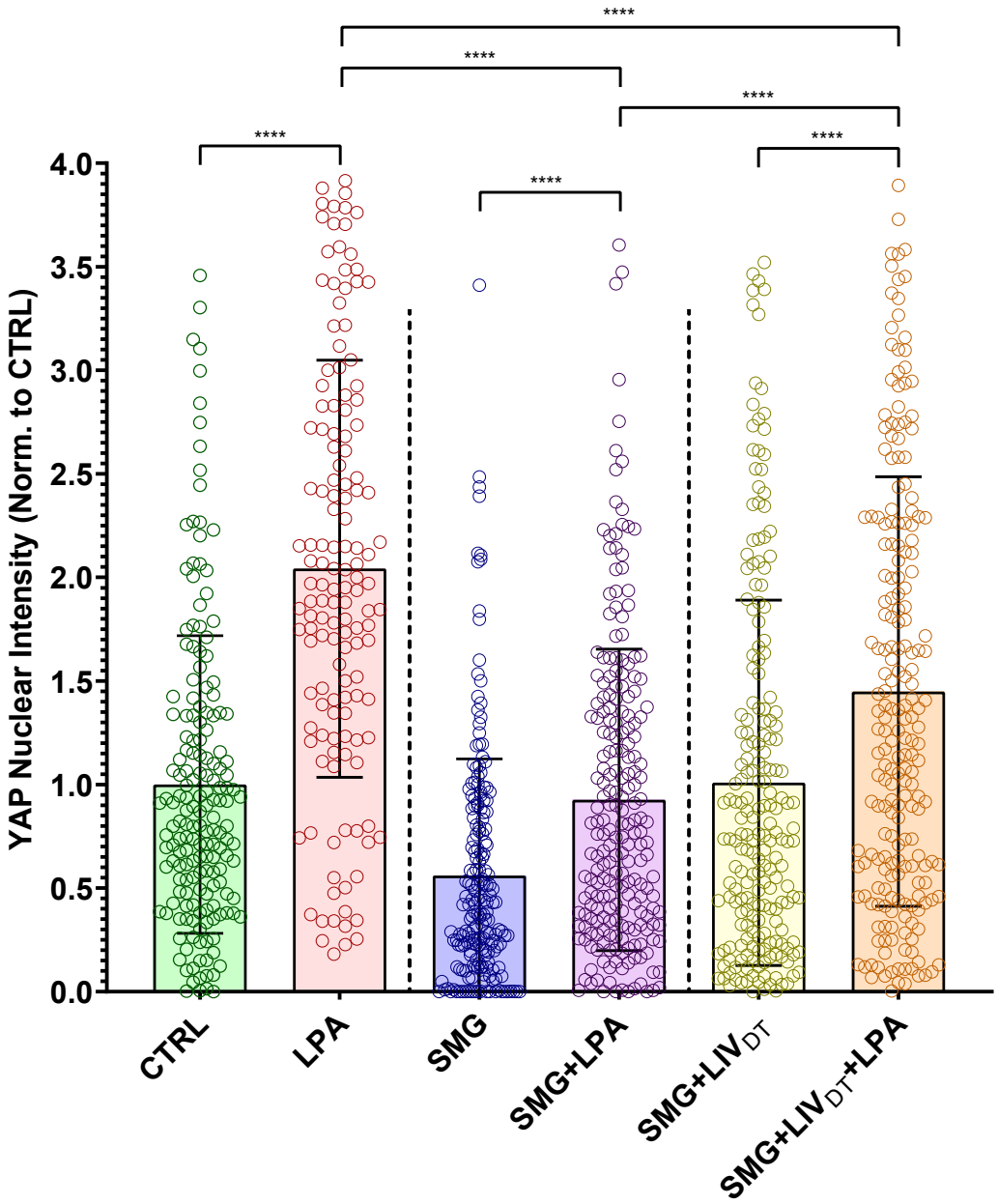

Figure 6. LPA-induced YAP nuclear entry decreased by SMG was alleviated by daily LIV$_{DT}$ application. MSCs were subjected to SMG, and parallel SMG+LIV$_{DT}$ over 72h period at the end of 72h, samples were treated with either LPA (50μM) or DMSO. Quantitative analysis of confocal images revealed that LPA addition increased nuclear YAP levels by 105%, 67% and 43% in the CTRL, SMG and SMG+LIV$_{DT}$ when compared to DMSO controls. When compared to nuclear YAP intensity of the LPA treatment alone, SMG+LPA and SMG+LIV$_{DT}$+LPA samples were 55% and 29% lower, respectively. YAP nuclear levels in SMG+LIV$_{DT}$+LPA remained 70% higher than SMG+LPA group. n>100/grp. Group comparisons were made via Kruskal-Wallis test followed by Tukey multiple comparison, *p<0.05, **p<0.01, ***p<0.01, ****p<0.0001.

Figure 7.

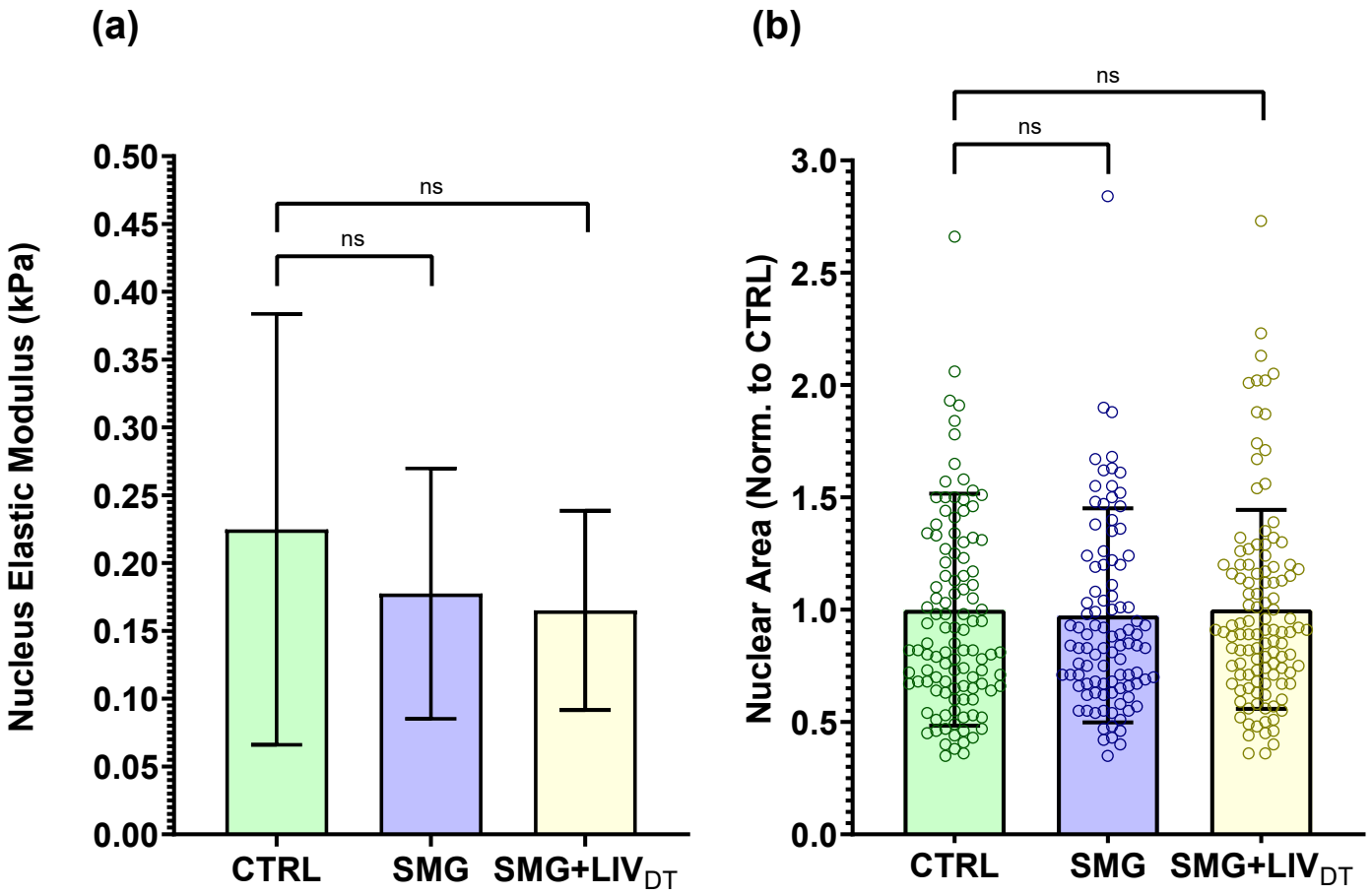

Figure S1. LINC complex disruption decreases nuclear YAP levels and reduces LIV$_{AT}$-induced YAP nuclear entry. Plasmids harboring either a dominant negative KASH domain of Nesprin (DNK) to disable LINC complex function or empty mCherry control (MC) were overexpressed in MSCs. Following puromycin selection, MC or DNK expressing MSCs were subjected to LIV$_{AT}$. Quantitative analysis of confocal images revealed a 49% increase of nuclear YAP following LIV$_{AT}$ in MC expressing control MSCs. Basal YAP levels of the DNK-CTRL group was 34% lower compared to MC-CTRL and LIV$_{AT}$ treatment failed to significantly increase nuclear YAP over DNK-CTRL (18%, NS). n=30/grp, group comparisons were made via Kruskal-Wallis test followed by Tukey multiple comparison, *p<0.05, **p<0.01, ***p<0.01, ****p<0.0001.

Supplementary Information

Low Intensity Vibration Restores Nuclear YAP Levels and Acute YAP Nuclear Shuttling in Mesenchymal Stem Cells Subjected to Simulated Microgravity

Thompson M[1], Woods K[2], Newberg, J[1], Oxford JT, Uzer G[1†]

[1]Mechanical and Biomedical Engineering, Boise State University
[2]Biomolecular Sciences Graduate Program, Boise State University
[†] Corresponding Author

Funding support:
NASA ISGC NNX15AI04H, NIH R01AG059923, and 5P2CHD086843-03, P20GM109095, P20GM103408 and NSF 1929188.

Figure S1.

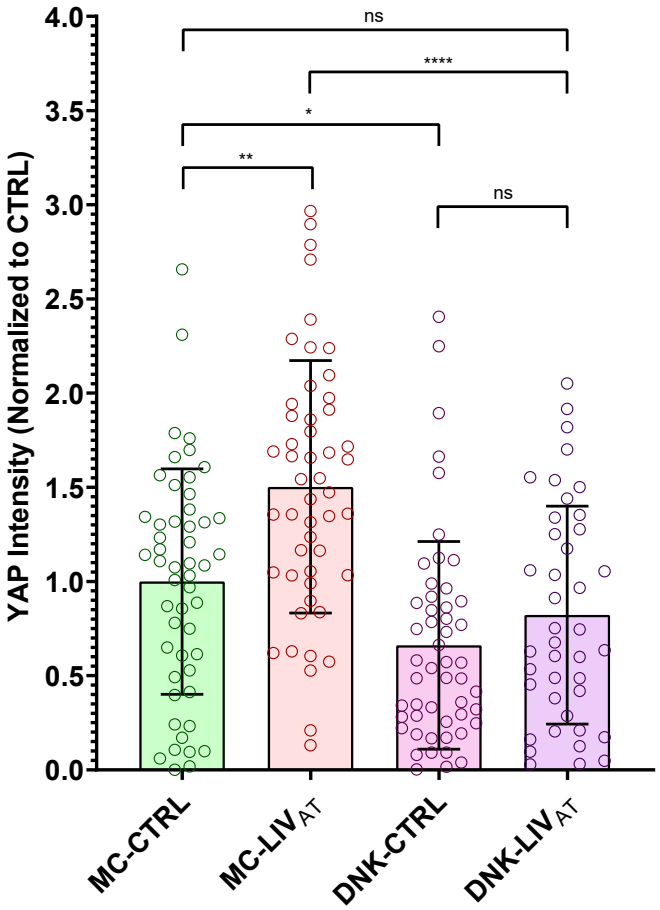

Figure S1. LINC complex disruption decreases nuclear YAP levels and reduces LIV$_{AT}$-induced YAP nuclear entry. Plasmids harboring either a dominant negative KASH domain of Nesprin (DNK) to disable LINC complex function or empty mCherry control (MC) were overexpressed in MSCs. Following puromycin selection, MC or DNK expressing MSCs were subjected to LIV$_{AT}$. Quantitative analysis of confocal images revealed a 49.27% increase of nuclear YAP following LIV$_{AT}$ in MC expressing control MSCs. Basal YAP levels of the DNK-CTRL group was 33.91% lower compared to MC-CTRL and LIV$_{AT}$ treatment failed to significantly increase nuclear YAP over DNK-CTRL (18.33%, NS). n=30/grp, group comparisons were made via Kruskal-Wallis test followed by Tukey multiple comparison, *p<0.05, **p<0.01, ***p<0.01, ****p<0.0001.